PCCP

Dynamic Article Links ►

Cite this: DOI: 10.1039/c0xx00000x

www.rsc.org/xxxxxx

COMMUNICATION

Structural and spectroscopic characterization of potassium fluoroborohydrides

Richard H. Heyn,*[a] Ivan Saldan,[b#] Magnus H. Sørby,[b] Christoph Frommen,[b] Bjørnar Arstad,[a] Aud M. Bougza,[a] Helmer Fjellvåg,[c] and Bjørn C. Hauback[b]

Received (in XXX, XXX) Xth XXXXXXXXX 20XX, Accepted Xth XXXXXXXXX 20XX
DOI: 10.1039/b000000x

Mechanochemical reactions between KBH_4 and KBF_4 result in the fluorinated potassium fluoroborohydride $K(BH_xF_{4-x})$ (x = 0-4), as determined by ^{11}B and ^{19}F solid state NMR. The materials maintain the cubic KBH_4 structure. Thermogravametric (TG) data for a ball-milled sample with KBH_4:KBF_4 = 3:1 is consistent with only desorption of hydrogen.

Metal borohydrides are intensively investigated in the context of energy storage due to their high hydrogen content.[1] Recently, there has also been reported high Li-ion conductivity in several Li-containing borohydrides, such as ortho-$LiBH_4$[2] and $LiCe(BH_4)_3Cl$,[3] which makes them interesting as solid electrolytes in Li-ion batteries. Partial substitution of the tetraborohydride anions (BH_4^-) with heavy halides (Cl^-, Br^- or I^-) has been successfully used to alter the properties of borohydrides, e.g. to stabilize the Li-conducting, high-temperature ortho-$LiBH_4$ phase at room temperature.[4-8] However, the inclusion of heavy halides has only a minor effect on the temperature of hydrogen desorption,[9,10] which must be significantly lowered for alkali- and alkaline earth borohydrides to become viable hydrogen storage materials. For alanates, substitution of hydrogen with fluorine has shown a large effect on the thermal stability,[11] and substitution of F^- anions into $LiBH_4$ has been recently shown theoretically to result in materials with favorable thermodynamics for onboard hydrogen storage applications.[12] Despite the chemical similarity between hydrides and fluorides, there is only one report of confirmed fluorine substitution in borohydrides.[13] An earlier report only presumes the formation of a fluoroborohydride.[14]

The present paper reports the results from ball milling of mixtures of KBH_4 and KBF_4 in the molar ratios 3:1 and 1:1 (samples **1** and **2**, respectively). The mixtures were milled for 10 hours at ambient temperature. The powder X-ray diffraction (PXD) patterns of the milled products resembled that for pure KBH_4 ($CsClO_4$-type structure, space group *Fm*-3*m*), but with appreciable shifts in the Bragg peak positions to lower angles, thus indicating expansion of the unit cells. This is consistent with substitution of larger BF_4^- tetrahedra for BH_4^- tetrahedra or larger fluorine atoms for hydrogen. No Bragg peaks for KBF_4 (orthorhombic, $BaSO_4$-type structure) were observed.

The PXD data were analysed using the Rietveld method. The Rietveld fits for **1** and **2** are shown in Figures 1 and 2, respectively. The KBH_4 structure[15] was taken as the starting point. The K and B sublattices together form a NaCl-type structure. The B positions are cubically coordinated by 8 half-occupied H positions, representing a disordered distribution of two orientations of the tetrahedral BH_4^- ions related by a 90° rotation. To allow for fluorine substitution in the model, an additional site was added to give a cubic configuration of empty fluorine sites, initially coinciding with the H sites, around the boron atoms. The occupation of the H and F sites were refined with the constraint that the sum should remain ½, i.e. the B atoms should remain 4-coordinated. The position of the H atoms was fixed at the expected B-H distance of 1.1 Å and not refined due to the minuscule scattering length of hydrogen. The position of the F site was refined to account for the difference in bond length between B-H and B-F. The results of the refinements are presented in Table 1. The unit cell parameters of **1** and **2** were 6.8174(2) Å and 6.9219(9) Å, respectively, compared to 6.7280(8) Å for pure KBH_4.[15] Thus, the unit cell *a* axis increases linearly with the amount of fluorine in the sample; this is consistent with the existence of a solid solution. Moreover, the refined compositions of the 3:1 and 1:1 phases are close to the nominal compositions (see Table 1). Refinements with the phase compositions fixed at the nominal compositions gave little or no change in the R-factor (R_{wp} = 4.86% for **1** and unchanged for **2**). These findings point towards a complete incorporation of the fluoride into the KBH_4 phase; the nominal compositions are therefore used in the ensuing discussions.

Table 1 Results from Rietveld refinements from PXD data.

Sample	$3KBH_4 + KBF_4$, **1**	$KBH_4 + KBF_4$, **2**
Nominal composition	KBH_3F	KBH_2F_2
Unit cell axis (a)	6.8174(2) Å	6.9219(9) Å
Refined composition	$KBH_{2.77(2)}F_{1.23(2)}$	$KBH_{1.79(7)}F_{2.21(7)}$
Z	4	4
Formula weight	76.06 g/mol	93.70 g/mol
F in *32f* (x,x,x)	x = 0.621(5)	x = 0.608(8)
R_{wp}, χ^2	4.77%, 1.96	11.6%, 1.49

[a] Space group *Fm*-3*m*. K in *4q* (0 0 0). B in *4b* (½ ½ ½), H in *32f* (0.59 0.59 0.59).

The PXD measurements cannot determine whether **1** and **2** contain discrete BH_4^- and BF_4^- anions or both H and F are bonded to the same B atom. To clarify this, the samples were studied by ^1H, ^{11}B and ^{19}F solid state NMR spectroscopy and compared to the spectra of the KBH_4 and KBF_4 standards. Figure 3 shows the ^{11}B NMR spectra for **1**, **2**, and the starting materials. Both **1** and **2**

show two peaks near -0.5 and -38 ppm, consistent with the single peaks observed for KBF_4 and KBH_4, respectively. The Multiple Quantum Magic Angle Spinning (3QMAS) spectrum of **1** in Figure 4 shows that the -0.5 signal is composed of one major part and several smaller components, while the signal at -38 ppm is composed of four similar signals. These data are highly suggestive of a composition for **1** represented as KBH_xF_{4-x} (x = 0-4), in which the BF_4^- (x = 0) signal is localized at ~0 ppm and the – 38 signal consists of BHF_3^-, $BH_2F_2^-$, BH_3F^- and BH_4^- species. Further support for this formulation comes from H-B Cross Polarization (CP) and F-B CP spectra for **2**, as shown in Figure 5. These data show that the signal at ~0 ppm has no interaction with H at short contact times, while F has coupling to both signals..

The ^{19}F spectra for **1** and **2** support the formulation derived from the ^{11}B NMR data, that **1** and **2** are mixtures of $[BH_xF_{4-x}]^-$ tetrahedra. Figure 6 shows the ^{19}F spectra for **1**, **2**, and KBF_4, while Figure 7 shows the curve fitting of the ^{19}F spectra for **1** and **2**. Comparison of the ^{19}F spectra at different MAS speeds identified the spinning side bands and indicated that the signals in the region of -135 to -163 ppm were the isotropic signals. The curve fitting shows that the major peak in both **1** and **2** is at -152 ppm, consistent with the signal observed for pure KBF_4. The observed signals for **1** can be fitted with 7 distinct peaks, while those for **2** can be accounted for by 6 different peaks. While the number of fitted peaks are greater than that expected *a priori* from a mixture of KBH_3F, KBH_2F_2, $KBHF_3$, and KBF_4, the 3QMAS data in Figure 4 indicates at least seven B-containing components – three in the 0 ppm region and four in the -38 ppm region – if all minor peaks are taken into account. Regardless of the actual identity of all the signals in the ^{11}B and ^{19}F NMR spectra, the overall results are much more consistent with a formulation consisting of a distribution of $[B(H,F)_4]^-$ tetrahedra rather than discreet, yet intermixed, BH_4^- and BF_4^- tetrahedra.

The results of TG experiments for **1** and **2** are shown in Figure 8. The TG curve for **1** shows a weight loss of about 3 % in the temperature region between 400 ^oC and 500 ^oC. This weight loss is consistent with complete desorption of hydrogen. Above 500 ^oC the TG curve is flat. Compared to the ball milled starting materials, **1** decomposes about 50 ^oC lower than pure KBF_4 and about 160 ^oC lower than pure KBH_4,[17] consistent with theoretical predictions.[11] In contrast to **1**, the TG curve for **2** shows several steps for the thermal decomposition. About a 2 wt % loss is observed between 400 and 500 ^oC, and an additional 4.5 weight % is lost between 500 ^oC and 600 ^oC. Above 600 ^oC, the TG curve continues to "creep," resulting in a total mass loss of about 10% between RT and 800 ^oC. While the initial weight loss may be due to hydrogen desorption, the remaining loss is probably a result of the higher fluorine content of **2** compared to **1**, leading to a continuous release of BF_3 and related species at higher temperatures.

The potential of **1** for reversible hydrogen sorbtion was assessed by a desorption-rehydrogenation experiment. First, **1** was desorbed at 520 $^\circ C$ under dynamic vacuum. It was then rehydrogenated at 350 $^\circ C$ under 100 bar of H_2 backpressure. TG experiments on the as-milled, desorbed and rehydrogenated samples were performed and are presented in Figure 9. Whereas the ball-milled mixture released about 2.7 wt.%, the sample after desorption and after rehydrogenation show identical behavior with no apparent mass loss up to 550 $^\circ C$, indicating that the system is irreversible.

The original report[13] for the synthesis of the material assigned as KBH_3F involved reaction of KF with diborane in dimethoxyethane (DME) at room temperature. The isolated material showed acceptable elemental analysis and a PXD pattern with "some lines ... coincident with KBH_4". Our efforts to reproduce this reaction utilized nearly equimolar amounts of KF and $BH_3{\bullet}SMe_2$ in refluxing DME. Reactions at room temperature even for extended periods did not lead to complete reaction of the starting materials. PXD of the material obtained after overnight reflux, **3**, showed the presence of both KBH_4 and KBF_4, some residual KF, and other, unidentified products (Figure 3S). While the solid state ^{11}B NMR spectrum of **3** is also consistent with the presence of BH_4^- and BF_4^- tetrahedra, the peaks are quite narrow, indicative of small quadrupolar couplings and a symmetric local environment. The ^1H NMR spectra for **1** – **3** (Figure 6S) is also consistent with a more symmetric local environment for **3**, with a narrower peak and a distinct lack of spinning side bands in comparison to the ^1H spectra for **1** and **2**. Additionally, like **1** and **2**, the ^{19}F NMR spectrum of **3** shows a resonance at -152.5, which is again consistent with the presence of KBF_4. The NMR data clearly support, therefore, the formation of $[BH_xF_{4-x}]^-$ tetrahedra during ball-milling but a complete redistribution reaction in solution yielding discrete phases of KBH_4 and KBF_4.

In summary, ball milling mixtures of KBH_4 and KBF_4 gives rise to a mixed fluoroborohydride solid of the composition $K(BH_xF_{4-x})$ (x = 0 - 4), that crystallises in a cubic, KBH_4-like lattice. An increase in unit cell dimensions is observed upon increasing F content, consistent with the presence of more F within the KBH_4-like lattice. The characterization of these new fluoroborohydride material phases is supported by solid state ^{11}B and ^{19}F NMR and TG data. 3QMAS and CP spectra collected on **1** and **2** show the interaction between F and B in both the BF_4^- - like peak at ~0 ppm and the BH_4^- - like peak at -38 ppm. The incorporation of F^- into borohydrides decreases the overall decomposition temperature, consistent with theoretical predictions.[12] Experiments to determine the homogeneity range of these fluoroborohydride phases, the mechanism of the H_2 desorption, and extension of this work to other alkali metal borohydrides is ongoing and will be published in due course.

Acknowledgements

The authors would like to thank the NANOMAT program of the Research Council of Norway for financial support and Ms. Vanessa Lelevrier (Erasmus program, University of Rennes, France) for NMR data acquisition.

Notes and references

[a] *SINTEF Materials and Chemistry, P. O. Box 124 Blindern, 0314 Oslo, Norway. Fax: +47 7359 7043; Tel: +47 9824 3927; E-mail: rhh@sintef.no*

[b] *Institute for Energy Technology (IFE), P. O. Box 40, 2027 Kjeller, Norway.*

[c] *Department of Chemistry, University of Oslo, P. O. Box 1033 Blindern, 0315 Oslo, Norway.*

[#] *Current address: Department of Physical and Colloid Chemistry, Chemical Faculty,Ivan Franko National University of Lviv,6 Kyryla and Mefodiya Str., UA-79005, Lviv, Ukraine*

† Electronic Supplementary Information (ESI) available: Experimental details of ball milling and wet chemical syntheses and the PXD, NMR, and TG experiments. Solid state ^{11}B and ^{19}F NMR spectra and PXRD pattern of **3**. Enlarged views of Figures 3 and 6. ^{1}H NMR spectra for **1** . **3**. See DOI: 10.1039/b000000x/

1. H. W. Li, Y. G. Yan, S. Orimo, A. Zuttel and C. M. Jensen, *Energies* 2011, **4**, 185-214.
2. M. Matsuo, Y. Nakamori, S. Orimo, H. Maekawa and H. Takamura, *Appl. Phys. Lett.*, 2007, **91**, 224103.
3. M. B. Ley, D. B. Ravnsbæk, Y. Filinchuk, Y.-S. Lee, R. Janot, Y. W. Cho, J. Skibsted and T. R. Jensen, *Chem. Mater.*, 2012, **24**, 1654-1663.
4. L. M. Arnbjerg, D. B. Ravnsbaek, Y. Filinchuk, R. T. Vang, Y. Cerenius, F. Besenbacher, J. E. Jorgensen, H. J. Jakobsen and T. R. Jensen, *Chem. Mater.*, 2009, **21**, 5772-5782.
5. H. Maekawa, M. Matsuo, H. Takamura, M. Ando, Y. Noda, T. Karahashi and S. I. Orimo, *J. Am. Chem. Soc.*, 2009, **131**, 894-895.
6. M. Matsuo, H. Takamura, H. Maekawa, H. W. Li and S. Orimo, *Appl. Phys. Lett.*, 2009, **94**, 084103.
7. R. Miyazaki, T. Karahashi, N. Kumatani, Y. Noda, M. Ando, H. Takamura, M. Matsuo, S. Orimo and H. Maekawa, *Solid State Ionics*, 2011, **192**, 143-147.
8. H. Oguchi, M. Matsuo, J. S. Hummelshoj, T. Vegge, J. K. Norskov, T. Sato, Y. Miura, H. Takamura, H. Maekawa and S. Orimo, *Appl. Phys. Lett.*, 2009, **94**, 141912.
9. S. Hino, J. E. Fonnelop, M. Corno, O. Zavorotynska, A. Damin, B. Richter, M. Baricco, T. R. Jensen, M. H. Sørby and B. C. Hauback, *J. Phys. Chem. C*, 2012, **116**, 12482-12488.
10. J. E. Olsen, M. H. Sørby and B. C. Hauback, *J. Alloys Comp.*, 2011, **509**, L228-L231.
11. H. W. Brinks, A. Fossdal and B. C. Hauback, *J. Phys. Chem. C*, 2008, **112**, 5658-5661.
12. L. Yin, P. Wang, Z. Fang and H. Cheng, *Chem. Phys. Lett.*, 2008, **450**, 318-321.
13. V. D. Aftandilian, H. C. Miller and E. L. Muetterties, *J. Am. Chem. Soc.*, 1961, **83**, 2471-2474.
14. H. I. Schlesinger, H. C. Brown, J. R. Gilbreath and J. J. Katz, *J. Am. Chem. Soc.*, 1953, **75**, 195-199.
15. R. L. Luck and E. J. Schelter, *Acta Cryst. C*, 1999, **55**, IUC9900151.
16. As an example of the relative insensitivity of the solid state ^{11}B NMR peak for BF_4^- anions upon changes in its chemical environment, contra that of BH_4^-, the chemical shift of $CsBF_4$ is -0.85 ppm and that of $CsBH_4$ is -28.2 ppm. R. H. Heyn, unpublished results.
17. S. Orimo, Y. Nakamori and A. Zuttel, *Mater. Sci. Engin. B*, 2004, **108**, 51-53 and references therein.
18. M. Corno, E. Pinatel, P. Ugliengo, M. Baricco, *J. Alloys Comp.*, 2011, **509S**, S679-S683.

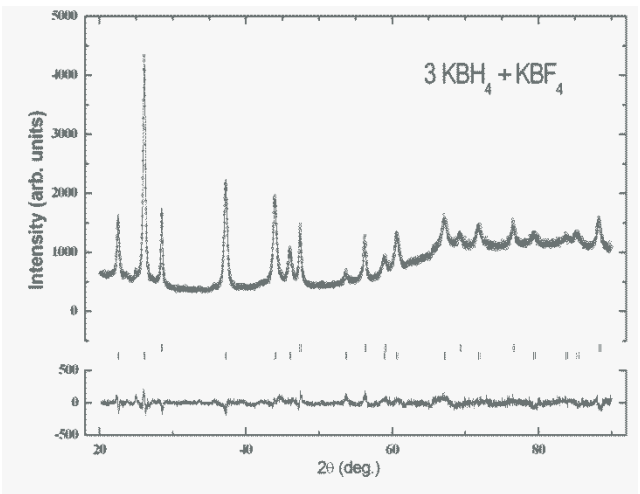

Fig. 1 Rietveld fit to PXD data for **1**. Open circles - experimental data, solid line - calculated data, below - difference plot. Vertical ticks mark the Bragg peak positions for Si (top) and KBH_3F (bottom). R_{wp} = 4.77% Cu Kα radiation

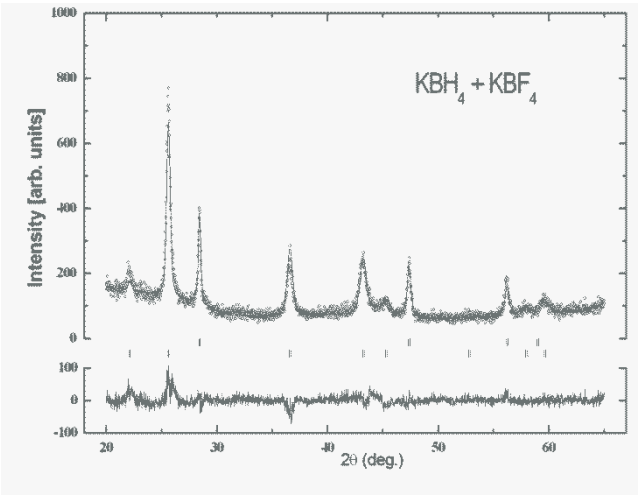

Fig. 2 Rietveld fit to PXD data for **2**. Open circles - experimental data, solid line - calculated data, below - difference plot. Vertical ticks mark the Bragg peak positions for Si (top) and KBH_2F_2 (bottom). R_{wp} = 11.6 % Cu Kα radiation

Fig.3 Solid state ^{11}B NMR spectra for, from top to bottom, KBH_4, KBF_4, **1**, and **2**.

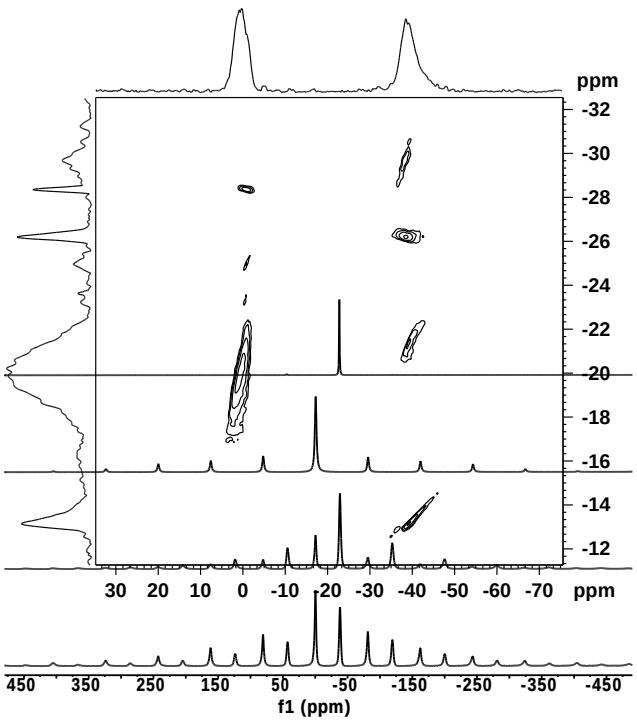

Fig.4 ^{11}B 3QMAS NMR spectrum for **1**.

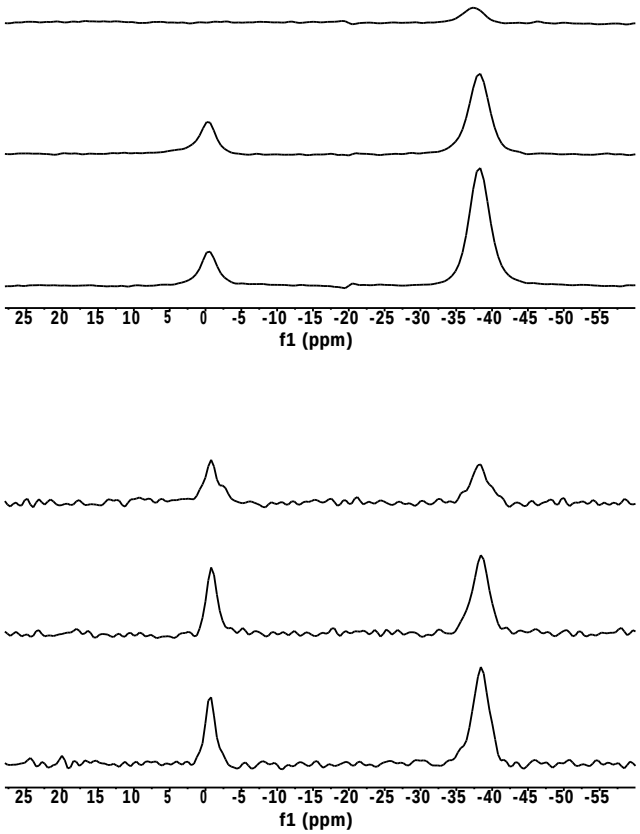

Fig.5 CP experiments on **2**. ^{1}H-^{11}B CP/MAS NMR (top) and ^{19}F-^{11}B (bottom). Contact times were (from top to bottom in each figure) 500, 1500, and 2000 ms.

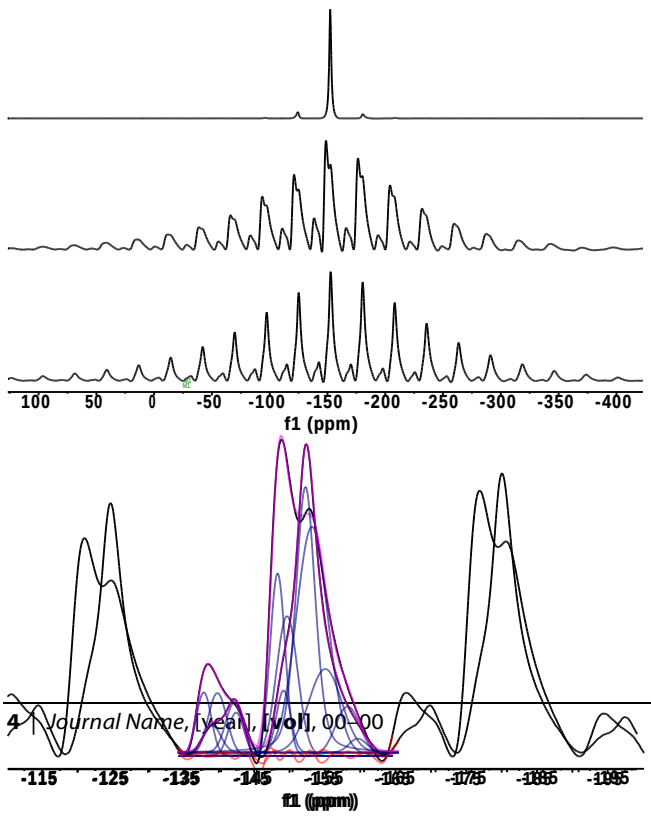

Fig.6 Solid state ^{19}F NMR spectra for, from top to bottom, KBF_4, **1**, and **2**. Experiments with variable MAS speeds shows that the isotropic signals are in the region -135 to -162 ppm.

Fig.7 Curve fitted ^{19}F MAS NMR spectra for **1** (top) and **2** (bottom). The asterisk indicates the -152 ppm peak, which is the same shift value as observed for the KBF_4 standard.

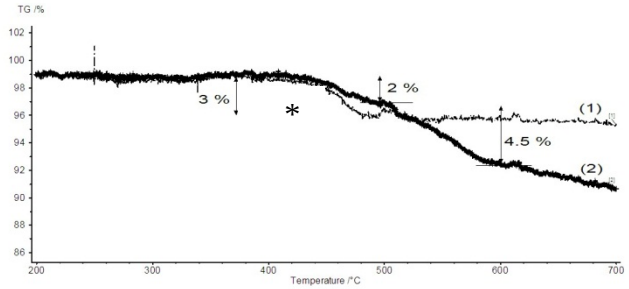

Fig. 8 TG curves for **1** and **2**.

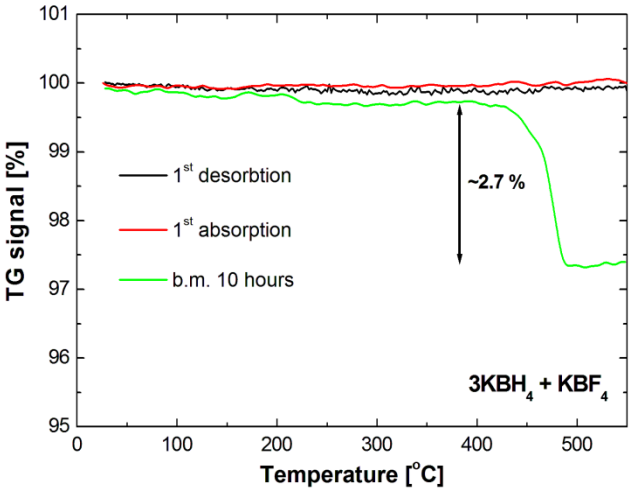

Fig. 9. TG curves for **1**, desorbed **1**, and **1** after attempted resorption of H_2.

Broader context

For realization of on-board hydrogen storage systems based on lightweight metal hydrides, specifically borohydrides, materials with better thermodynamic properties have to be synthesized. One potential route to improving the hydrogen desorption thermodynamics is to selectively replace part of the hydrogen with fluorine. While this has been shown to be a successful strategy *in silico*, the actual synthesis of well-described F-containing borohydrides has thus far not been realized. In this paper we show how ball milling mixtures of KBH_4 and KBF_4 results in new phases where the BF_4^- tetrahedron are constrained

in the cubic KBH_4 lattice. These new phases show lower hydrogen desorption temperatures than KBH_4. This work establishes an entry into a new class of materials for the further development of material solutions for on-board hydrogen storage.